

Conversion from W to Greenberger-Horne-Zeilinger states in the Rydberg-blockade regime of neutral-atom systems: Dynamical-symmetry-based approach

Thorsten Haase, Gernot Alber, and Vladimir M. Stojanović

Institut für Angewandte Physik, Technical University of Darmstadt, D-64289 Darmstadt, Germany

(Dated: March 24, 2021)

We investigate the possibilities for a deterministic conversion between two important types of maximally entangled multiqubit states, namely, W and Greenberger-Horne-Zeilinger (GHZ) states, in the Rydberg-blockade regime of a neutral-atom system where each atom is subject to four external laser pulses. Such interconversions between W states and their GHZ counterparts have quite recently been addressed using the method of shortcuts to adiabaticity, more precisely techniques based on Lewis-Riesenfeld invariants [R.-H. Zheng *et al.*, Phys. Rev. A **101**, 012345 (2020)]. Motivated in part by this recent work, we revisit the W to GHZ state-conversion problem using a fundamentally different approach, which is based on the dynamical symmetries of the system and a Lie-algebraic parametrization of its permissible evolutions. In contrast to the previously used invariant-based approach, which leads to a state-conversion protocol characterized by strongly time-dependent Rabi frequencies of external lasers, ours can also yield one with time-independent Rabi frequencies. This feature makes our protocol more easily applicable experimentally, with the added advantage that it allows the desired state conversion to be carried out in a significantly shorter time with the same total laser pulse energy used.

I. INTRODUCTION

Recent years have witnessed considerable progress in quantum-state engineering in a variety of physical systems [1–3], this being one of the essential prerequisites for the development of future quantum technologies [4, 5]. In particular, the recent milestones pertaining to the scalability of neutral-atom arrays trapped in optical tweezers [6–11] have reinvigorated interest in quantum-state engineering in ensembles of Rydberg atoms [12, 13]. These developments [14–19], in turn, bode well for future progress in the realm of quantum-information processing (QIP) with this class of atomic systems [20, 21], a research direction whose overarching goal is the realization of a neutral-atom quantum computer [22, 23]. High-fidelity state preparation/readout, quantum logic gates, and controlled quantum dynamics of more than 50 qubits have already been demonstrated in those systems, with the prospect of reliable QIP with hundreds of qubits being within reach [24].

Maximally-entangled multi-qubit states are of particular importance for QIP, regardless of the specific physical platform. Prominent ones among them are W [25] and Greenberger-Horne-Zeilinger (GHZ) [26] states, two classes of states that cannot be transformed into each other through local operations and classical communication (LOCC-inequivalence [27]). Owing to their favorable properties, both classes have proven useful in various QIP protocols [28–30], which triggered a large number of proposals for the preparation of W [31–39] and GHZ states [2, 40–43] in various systems.

Aside from tailored schemes for the preparation of W or GHZ states, which typically involve a simple product state as their point of departure [16], the interconversion between a W state and its GHZ counterpart represents another interesting problem of quantum-state engineering. The earliest attempt in this direction pertained to

a photonic system and was probabilistic in nature [44]. This pioneering study was followed by a further work with photons [45] and a study of analogous interconversions in a spin system [46]. Finally, irreversible conversions of a W state into a GHZ state were also proposed in the realm of atomic systems [47, 48].

Quite recently, deterministic interconversions between W and GHZ states have been investigated in the Rydberg-blockade (RB) regime [49, 50] of a neutral-atom system subject to four external laser pulses [17]. Each atom in this system was assumed to represent an effective two-level system, with the two relevant states (ground- and a Rydberg state) playing the roles of logical qubit states. This recent work was based on the method of shortcuts to adiabaticity (STA) [51]. More specifically yet, it utilizes the concept of Lewis-Riesenfeld invariants [52], in this case applied to an effective four-level Hamiltonian of the system. RB, the phenomenon whereby the van der Waals (vdW) interaction prevents simultaneous Rydberg excitation of more than one atom within a certain radius, represents the enabling physical mechanism for QIP with neutral atoms [22] as it engenders a conditional logic that permits the realization of entangling two-qubit gates [53–55]. From the point of view of quantum-state engineering, the most important implication of RB is that it leads to the creation of coherent superpositions with a single Rydberg excitation being shared among all atoms in an ensemble [54]. Such superpositions are maximally-entangled states of W type [56].

In this paper, we study the conversion of an initial W state into a GHZ state in the same physical setting as Ref. [17] – i.e., the RB regime of a system of neutral atoms interacting through vdW interactions. However, we employ a fundamentally different approach than that of Ref. [17]. Namely, our approach entails the use of the dynamical symmetries [57, 58] of the system under consideration and is mathematically framed using the lan-

guage of Lie algebras. Another important technical ingredient of our approach is a particular parametrization of all the unitary transformations connecting arbitrary two states of the four-dimensional representation of the Lie algebra $so(4)$ [59]. We utilize this parametrization to describe the dynamics corresponding to the effective system Hamiltonian that depends on the aforementioned Rabi frequencies. We then single out specific unitary evolutions of the system that connect the initial- and final states (W and GHZ, respectively) in the quantum-state control problem at hand. This allows us to determine the corresponding Rabi frequencies of external laser pulses.

In contrast to the STA-based approach of Ref. [17], which results in a state-conversion protocol characterized by time-dependent Rabi frequencies with a rather complex time dependence, our approach can also yield one with constant (i.e., time-independent) Rabi frequencies. Importantly, this last feature makes our resulting protocol more easily applicable experimentally than that of Ref. [17], with the added benefit that it allows the desired state conversion to be carried out in a significantly shorter time.

The remaining part of this work is organized in the following manner. In Sec. II we introduce the Rydberg-atom system under consideration, specifying at the same time the notation and conventions to be used throughout the paper. In Sec. III we lay the groundwork for our dynamical-symmetry-based approach, with emphasis on its Lie-algebraic description. Section IV is concerned with the Hamiltonian dynamics, first in the most general case and then under the constraints inherent to the model used. In Sec. V we first discuss the specific unitary evolutions of the system that are required for carrying out the desired state conversion. We then determine the corresponding Rabi frequencies. Finally, we compare our resulting state-conversion protocol with the one obtained in Ref. [17], with emphasis on the robustness of those protocols against decoherence effects. We close in Sec. VI with a summary of the results and questions for future work. Some involved mathematical details are relegated to Appendices A and B.

II. SYSTEM AND EFFECTIVE HAMILTONIAN

We consider a system that consists of three equidistant and identical neutral atoms in the RB regime [for an illustration, see Fig. 1(a)]. All three atoms are subject to the same four external laser pulses, with their corresponding Rabi frequencies being denoted by Ω_{r0} , Ω_{r1} , Ω_{r2} , and Ω_{r3} . These pulses, with frequencies ω_i ($i \in \{0, 1, 2, 3\}$), are close to being resonant with only a single internal (electronic) transition $|g\rangle \leftrightarrow |r\rangle$. Thus, each atom can effectively be treated as a two-level system with its electronic ground state $|g\rangle$ and a highly-excited Rydberg state $|r\rangle$. These states encode the logical $|0\rangle$ and $|1\rangle$ qubit states, respectively. Therefore, from the QIP standpoint this is a system of neutral-atom qubits

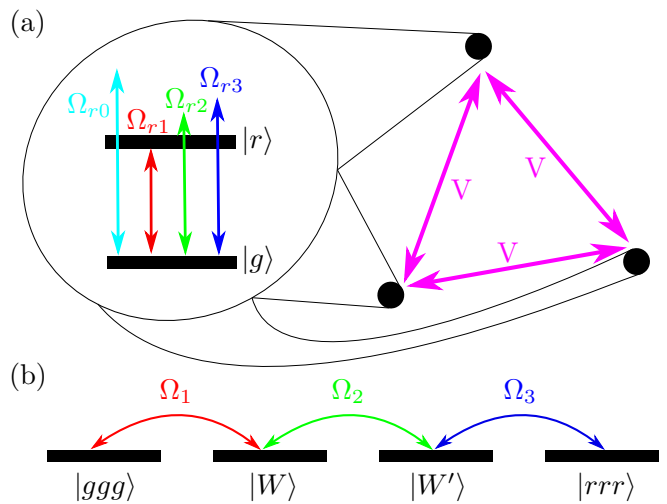


FIG. 1. (Color online)(a) Schematic of the system under consideration: Three identical neutral atoms with internal states $|g\rangle$ and $|r\rangle$ (gr -type qubits) and constant vdW interaction energy $\hbar V$, which are subject to four external laser pulses. (b) Pictorial illustration of the effective Hamiltonian H_{eff} in Eq. (3).

of the ground-Rydberg (gr) type [24]. Note that the typical energy splitting of such qubits in frequency units is (900 – 1500) THz (depending on the choice of atomic species and the Rydberg states used), thus in practice gr -qubit manipulations entail either an ultraviolet laser or a combination of visible and infrared lasers in a ladder configuration. Owing to their relatively straightforward initialization, manipulation, and measurement – as compared to other kinds of neutral-atom qubits – gr qubits currently represent the preferred qubit type for fast ($\lesssim 100$ ns) and high-fidelity entangling operations [21], as well as for quantum-state engineering [16].

The interaction-picture Hamiltonian of the system is given by

$$H_I(t)/\hbar = \sum_{k=1}^3 \sum_{i=0}^3 \Omega_{ri}(t) e^{-i(\delta_i + \Delta_i)t} |r\rangle_{kk} \langle g| + \text{H.c.} + \sum_{p < q} V |rr\rangle_{pq} \langle rr|. \quad (1)$$

Here, the laser frequencies are slightly detuned from the atomic transition frequency, i.e. $\omega_i = (E_r - E_g)/\hbar + \Delta_i + \delta_i$ with $i \in \{0, 1, 2, 3\}$. The Rabi frequencies Ω_{r1} , Ω_{r2} , and Ω_{r3} are time dependent and real-valued, while Ω_{r0} is time independent and plays the role of inducing appropriate quadratic Stark shifts. $\hbar V$ is the constant vdW interatomic interaction energy. The interatomic interaction between each pair of excited Rydberg atoms is described approximately by an energy shift of magnitude $\hbar V$ according to lowest order perturbation theory.

As shown in Ref. [17], by choosing the detunings δ_i and Δ_i appropriately, the system Hamiltonian can be reduced

via perturbation theory to an effective Hamiltonian defined in the manifold of four three-particle states $|ggg\rangle$, $|W\rangle = (|rgg\rangle + |grg\rangle + |ggr\rangle)/\sqrt{3}$, $|W'\rangle = (|rrg\rangle + |grr\rangle + |rgr\rangle)/\sqrt{3}$, and $|rrr\rangle$. To be more specific, choosing the detunings such that $\delta_0 = 0$, $\Delta_1 = 0$, $\Delta_2 = V$, $\Delta_3 = 2V$, and

$$\begin{aligned}\delta_1 &= -\frac{6\Omega_{r0}^2}{\Delta_0} + \frac{4\Omega_{r0}^2}{\Delta_0 - V}, \\ \delta_2 &= \frac{3\Omega_{r0}^2}{\Delta_0} - \frac{8\Omega_{r0}^2}{\Delta_0 - V} + \frac{3\Omega_{r0}^2}{\Delta_0 - 2V}, \\ \delta_3 &= \frac{4\Omega_{r0}^2}{\Delta_0 - V} - \frac{6\Omega_{r0}^2}{\Delta_0 - 2V},\end{aligned}\quad (2)$$

yields the effective Hamiltonian

$$H_{\text{eff}}(t)/\hbar = \Omega_1(t)|ggg\rangle\langle W| + \Omega_2(t)|W\rangle\langle W'| + \Omega_3(t)|W'\rangle\langle rrr| + \text{H.c.}, \quad (3)$$

where $\Omega_1(t) = \sqrt{3}\Omega_{r1}(t)$, $\Omega_2(t) = 2\Omega_{r2}(t)$, and $\Omega_3(t) = \sqrt{3}\Omega_{r3}(t)$.

In addition to the two-level approximation a sufficient set of conditions for the validity of this effective Hamiltonian requires sufficiently long interaction times T_{int} , i.e. $\min\{|\Delta_0|, |V|\}T_{\text{int}} \gg 1$, and $|\Delta_0|, |V| \gg |\Omega_{r0}|, \min\{|\delta_i|; i = 1, 2, 3\} \gg \max\{|\Omega_{ri}(t)|; i = 1, 2, 3\}$.

It is pertinent to comment at this point on the realm of applicability of the last effective Hamiltonian – as well as the ensuing state-conversion scheme – vis-à-vis the RB regime, as the latter represents the regime of primary interest for QIP with neutral atoms [22]. In this context it is useful to recall that the RB regime is defined as the one in which the interaction-induced energy shift $\hbar V$ is much larger than the Fourier-limited width of the laser pulses involved (i.e. $|V|T_{\text{int}} \gg 1$, where T_{int} is the pulse duration). Because this last condition is satisfied for all the laser pulses envisioned to be used in our present state-conversion scheme, we can identify the RB regime as the domain of applicability of our approach.

In the following it is demonstrated that just on the basis of the $so(4)$ dynamical symmetry of the last effective Hamiltonian alone, i.e. without invoking the Lewis-Riesenfeld method of Ref. [17], a simpler and more time-efficient protocol for the desired conversion of W states into their GHZ counterparts can be found.

III. DYNAMICAL SYMMETRIES

In what follows the $su(2) \oplus su(2) \cong so(4)$ dynamical symmetry of the effective Hamiltonian in Eq. (3) is investigated. It is shown that under the assumption of real-valued Rabi frequencies $\Omega_i(t)$ ($i = 1, 2, 3$) this last Hamiltonian describes the quantum dynamics of two constrained pseudospin-1/2 degrees of freedom.

To begin with, we map the orthonormal basis states in the Hamiltonian of Eq. (3) onto column vectors according

to

$$\begin{aligned}|ggg\rangle &\rightarrow \begin{pmatrix} 1 \\ 0 \\ 0 \\ 0 \end{pmatrix}, & |W\rangle &\rightarrow \begin{pmatrix} 0 \\ 1 \\ 0 \\ 0 \end{pmatrix}, \\ |W'\rangle &\rightarrow \begin{pmatrix} 0 \\ 0 \\ 1 \\ 0 \end{pmatrix}, & |rrr\rangle &\rightarrow \begin{pmatrix} 0 \\ 0 \\ 0 \\ 1 \end{pmatrix}.\end{aligned}\quad (4)$$

Within this notation the six matrices

$$\begin{aligned}S_1 &= \frac{1}{2} \begin{pmatrix} 0 & 1 & 0 & 0 \\ 1 & 0 & 0 & 0 \\ 0 & 0 & 0 & 1 \\ 0 & 0 & 1 & 0 \end{pmatrix}, & T_1 &= \frac{1}{2} \begin{pmatrix} 0 & 1 & 0 & 0 \\ 1 & 0 & 0 & 0 \\ 0 & 0 & 0 & -1 \\ 0 & 0 & -1 & 0 \end{pmatrix}, \\ S_2 &= \frac{1}{2} \begin{pmatrix} 0 & 0 & 0 & -1 \\ 0 & 0 & 1 & 0 \\ 0 & 1 & 0 & 0 \\ -1 & 0 & 0 & 0 \end{pmatrix}, & T_2 &= \frac{1}{2} \begin{pmatrix} 0 & 0 & 0 & 1 \\ 0 & 0 & 1 & 0 \\ 0 & 1 & 0 & 0 \\ 1 & 0 & 0 & 0 \end{pmatrix}, \\ S_3 &= \frac{1}{2} \begin{pmatrix} 0 & 0 & -i & 0 \\ 0 & 0 & 0 & i \\ i & 0 & 0 & 0 \\ 0 & -i & 0 & 0 \end{pmatrix}, & T_3 &= \frac{1}{2} \begin{pmatrix} 0 & 0 & -i & 0 \\ 0 & 0 & 0 & -i \\ i & 0 & 0 & 0 \\ 0 & i & 0 & 0 \end{pmatrix},\end{aligned}\quad (5)$$

with Lie brackets

$$\begin{aligned}[S_i, S_j] &= i\epsilon_{ijk}S_k, \\ [T_i, T_j] &= i\epsilon_{ijk}T_k, \\ [S_i, T_j] &= 0,\end{aligned}\quad (6)$$

constitute a four dimensional representation of the Lie algebra $su(2) \oplus su(2) \cong so(4)$ and thus describe two independent angular momenta. From the relevant Casimir operators

$$I = \sum_{i=1}^3 (S_i^2 + T_i^2) = \frac{3}{2}, \quad J = \sum_{i=1}^3 (S_i^2 - T_i^2) = 0 \quad (7)$$

it is apparent that the (dimensionless) two angular momentum operators with Cartesian components $\{S_i\}$ and $\{T_i\}$ ($i \in \{1, 2, 3\}$) describe two independent spin-1/2 degrees of freedom or pseudospins because $\sum_i S_i^2 = \sum_i T_i^2 = s(s+1)$ with $s = 1/2$. Furthermore, the matrices of the representation [cf. Eq. (5)] fulfill the additional relations

$$\begin{aligned}(2S_l)(2S_k) &= i\epsilon_{lkm}(2S_m) + \delta_{lk}, \quad l, k, m \in \{1, 2, 3\} \\ (2T_l)(2T_k) &= i\epsilon_{lkm}(2T_m) + \delta_{lk}\end{aligned}\quad (8)$$

in analogy to two commuting sets of Pauli spin matrices.

Provided the Rabi frequencies $\Omega_i(t)$ are real-valued the Hamiltonian of Eq. 3 is a linear combination of these angular momentum operators, i.e.

$$H_{\text{eff}}(t)/\hbar = \Omega_1(t)(S_1 + T_1) + \Omega_2(t)(S_2 + T_2) + \Omega_3(t)(S_1 - T_1). \quad (9)$$

This explicitly exhibits the Lie algebra $su(2) \oplus su(2)$ as the dynamical symmetry of this Hamiltonian [57, 58]. However, it is also apparent that this effective Hamiltonian is not the most general real-valued linear combination of the six independent operators S_i and T_i ($i \in \{1, 2, 3\}$). It is constrained by the fact that some operators, such $S_2 - T_2$, do not appear in this Hamiltonian.

In view of the $su(2) \oplus su(2)$ symmetry of the Hamiltonian (3) it is convenient to use the eigenstates of the spin operators of the two independent pseudospins as an orthonormal basis of the Hilbert space. These states can straightforwardly be constructed by starting from the common eigenvector of the operator $S_3 + T_3$ with the largest eigenvalue, i.e.

$$|\uparrow\uparrow\rangle \rightarrow \frac{1}{\sqrt{2}} \begin{pmatrix} -i \\ 0 \\ 1 \\ 0 \end{pmatrix} \quad (10)$$

with $(S_3 + T_3)|\uparrow\uparrow\rangle = |\uparrow\uparrow\rangle$. By applying the lowering operators $S_1 - iT_1$ and $T_1 - iT_2$ onto $|\uparrow\uparrow\rangle$ the remaining orthonormal states of the independent pseudospins are obtained, namely

$$\begin{aligned} |\uparrow\downarrow\rangle &\rightarrow \frac{1}{\sqrt{2}} \begin{pmatrix} 0 \\ -i \\ 0 \\ -1 \end{pmatrix}, \quad |\downarrow\uparrow\rangle \rightarrow \frac{1}{\sqrt{2}} \begin{pmatrix} 0 \\ -i \\ 0 \\ 1 \end{pmatrix}, \\ |\downarrow\downarrow\rangle &\rightarrow \frac{1}{\sqrt{2}} \begin{pmatrix} -i \\ 0 \\ -1 \\ 0 \end{pmatrix}. \end{aligned} \quad (11)$$

In this basis the angular momentum operators S_i (T_i) act on the first (second) pseudospin only. Therefore, these orthonormal basis states transform under an arbitrary unitary transformation in a simple way. In view of $[S_i, T_j] = 0$, $i, j \in \{1, 2, 3\}$ the most general unitary transformation generated by these commuting angular momenta can be written in the form

$$U(\boldsymbol{\alpha}, \boldsymbol{\beta}) = e^{-i\boldsymbol{\alpha} \cdot \mathbf{S}} e^{-i\boldsymbol{\beta} \cdot \mathbf{T}}. \quad (12)$$

Explicit expressions for the transformed pseudospin states of Eqs. (10) and (11) are given in Appendix A.

IV. UNITARY TRANSFORMATIONS AND TIME-DEPENDENT HAMILTONIANS

In this section basic properties of time-dependent unitary operators are discussed which are induced by time-dependent curves in the parameter space of the Lie algebra $su(2) \oplus su(2)$. Via the time-dependent Schrödinger equation their local properties are characterized by corresponding time-dependent Hamiltonians.

Let us consider a general time-dependent unitary transformation $U[\boldsymbol{\alpha}(t), \boldsymbol{\beta}(t)]$ as defined by Eq. (12) which

is induced by a time-dependent (differentiable) curve, say $\gamma : t \rightarrow \{\boldsymbol{\alpha}(t), \boldsymbol{\beta}(t)\}$ with $t \in [0, T]$, in the parameter space of the Lie algebra $su(2) \oplus su(2)$. Via the time-dependent Schrödinger equation such a time-dependent unitary transformation defines the corresponding time-dependent Hamiltonian $H(t)$, i.e.

$$i\hbar \frac{d}{dt} U[\boldsymbol{\alpha}(t), \boldsymbol{\beta}(t)] = H(t)U[\boldsymbol{\alpha}(t), \boldsymbol{\beta}(t)]. \quad (13)$$

This Hamiltonian $H(t)$ characterizes the local properties of this time evolution and is determined completely by the $su(2) \oplus su(2)$ commutation relations of Eq. (6). It can be determined in a straightforward way from Eq. (A1) of Appendix A, thus yielding the result

$$H(t)/\hbar = \boldsymbol{\omega}[\boldsymbol{\alpha}(t)] \cdot \mathbf{S} + \boldsymbol{\omega}[\boldsymbol{\beta}(t)] \cdot \mathbf{T} \quad (14)$$

with the time-dependent (vectorial) Rabi frequency

$$\begin{aligned} \boldsymbol{\omega}[\boldsymbol{\alpha}(t)] &= \frac{\sin |\boldsymbol{\alpha}(t)|}{|\boldsymbol{\alpha}(t)|} \dot{\boldsymbol{\alpha}}(t) + \frac{2 \sin^2 \frac{|\boldsymbol{\alpha}(t)|}{2}}{|\boldsymbol{\alpha}(t)|^2} [\boldsymbol{\alpha}(t) \times \dot{\boldsymbol{\alpha}}(t)] \\ &\quad + \frac{|\boldsymbol{\alpha}(t)| - \sin |\boldsymbol{\alpha}(t)|}{|\boldsymbol{\alpha}(t)|^3} [\boldsymbol{\alpha}(t) \cdot \dot{\boldsymbol{\alpha}}(t)] \boldsymbol{\alpha}(t) \end{aligned} \quad (15)$$

and with $\boldsymbol{\omega}[\boldsymbol{\beta}(t)]$ defined in an analogous fashion. [Note that here $\dot{\boldsymbol{\alpha}}(t)$ denotes the time derivative of $\boldsymbol{\alpha}(t)$.]

According to Eq. (14) each time dependent (differentiable) curve γ induces a time-dependent curve in the space of unitary transformations $U[\boldsymbol{\alpha}(t), \boldsymbol{\beta}(t)]$ whose associated time-dependent Hamiltonian $H(t)$ has the Lie algebra $su(2) \oplus su(2)$ as its dynamical symmetry. In general this time-dependent Hamiltonian $H(t)$ is a linear combination of all angular momenta of this Lie algebra. In the Hilbert space of the two pseudospins any pure quantum state, say $|\psi(0)\rangle$, can be converted into any other pure quantum state, say $|\psi(T)\rangle$, by the time-dependent Hamiltonian $H(t)$ of Eq. (14) provided a curve γ can be found with

$$\begin{aligned} U[\boldsymbol{\alpha}(0), \boldsymbol{\beta}(0)]|\psi(0)\rangle &= e^{i\Phi_0} |\psi(0)\rangle, \\ U[\boldsymbol{\alpha}(T), \boldsymbol{\beta}(T)]|\psi(0)\rangle &= e^{i\Phi_T} |\psi(T)\rangle. \end{aligned} \quad (16)$$

[Note that nonzero phases Φ_0, Φ_T are possible in Eq. (16) because pure quantum states are described by rays in Hilbert space.] If the form of the time-dependent Rabi frequencies of Eq. (15) are constrained by additional boundary conditions the possible curves γ in the parameter space of the Lie algebra $su(2) \oplus su(2)$ may be restricted so that particular quantum state conversions are no longer possible.

A typical example of a Hamiltonian with additional constraints is the effective time-dependent Hamiltonian of Eq. (3). Comparing Eqs. (9) and (14) these constraints are explicitly given by

$$\begin{aligned} \omega_3[\boldsymbol{\alpha}(t)] &= 0, \\ \omega_3[\boldsymbol{\beta}(t)] &= 0, \\ \omega_2[\boldsymbol{\alpha}(t)] - \omega_2[\boldsymbol{\beta}(t)] &= 0 \end{aligned} \quad (17)$$

and by the following relations

$$\begin{aligned}\Omega_1(t) &= \frac{\omega_1[\boldsymbol{\alpha}(t)] + \omega_1[\boldsymbol{\beta}(t)]}{2}, \\ \Omega_3(t) &= \frac{\omega_1[\boldsymbol{\alpha}(t)] - \omega_1[\boldsymbol{\beta}(t)]}{2}, \\ \Omega_2(t) &= \frac{\omega_2[\boldsymbol{\alpha}(t)] + \omega_2[\boldsymbol{\beta}(t)]}{2}\end{aligned}\quad (18)$$

which relate the components of the (vectorial) Rabi frequencies to the time-dependent parameters of Eq. (9). In particular, the relations (17) are anholonomic constraints that have to be fulfilled by all curves in the parameter space of the Lie algebra $su(2) \oplus su(2)$ which enable a pure state conversion with the aid of the effective Hamiltonian (3).

V. W-TO-GHZ QUANTUM STATE CONVERSION

In this section we address the question as to which effective state conversions between a W and a GHZ state are possible by appropriate choices of the time-dependent Rabi frequencies in the effective Hamiltonian of Eq. (3). In particular, it is demonstrated below that the $su(2) \oplus su(2)$ -based Lie-algebraic approach allows one to determine quantum state conversions which are significantly faster than the previously proposed STA-based protocol [17].

We are looking for time-dependent Rabi frequencies $\Omega_i(t)$ ($i = 1, 2, 3$) of the Hamiltonian [cf. Eq. (3)] that allow the conversion of an initially prepared W state into a GHZ state as described by Eq. (16) with

$$\begin{aligned}|\psi(0)\rangle &= |W\rangle, \\ |\psi(T)\rangle &= |\text{GHZ}\rangle = (|ggg\rangle + e^{i\varphi}|rrr\rangle) \frac{1}{\sqrt{2}}, \quad \varphi \in [0, 2\pi).\end{aligned}\quad (19)$$

For this purpose we have to find an appropriate curve γ in the parameter space of the Lie algebra $su(2) \oplus su(2)$ as described in Sec. IV whose induced unitary transformation $U[\boldsymbol{\alpha}(t), \boldsymbol{\beta}(t)]$ acts onto the initial state like the unit transformation at $t = 0$ and yields the final GHZ state at $t = T$. As this state conversion has to be achieved by the effective Hamiltonian (3) the time dependent Rabi frequencies have to fulfill the constraints (17) and the relations (18).

Let us first of all determine curves γ in the parameter space of $su(2) \oplus su(2)$ which fulfill the constraints (17). For the sake of simplicity we restrict our subsequent discussion to curves γ which fulfill the additional requirement that $|\boldsymbol{\alpha}(t)| = |\boldsymbol{\beta}(t)| = \pi$. In addition, expressing the vectorial parameters $\boldsymbol{\alpha}(t)$ and $\boldsymbol{\beta}(t)$ in spherical coordinates, i.e. $\alpha_1(t) = \pi \sin \theta_\alpha(t) \cos \phi_\alpha(t)$, $\alpha_2(t) = \pi \sin \theta_\alpha(t) \sin \phi_\alpha(t)$, $\alpha_3(t) = \pi \cos \theta_\alpha(t)$ and analogously for $\boldsymbol{\beta}(t)$, the anholonomic constraints of Eq. (17)

simplify to the relations

$$0 = \sin^2(\theta_\alpha(t)) \dot{\phi}_\alpha(t), \quad (20)$$

$$0 = \sin^2(\theta_\beta(t)) \dot{\phi}_\beta(t), \quad (21)$$

$$0 = \dot{\theta}_\alpha(t) \cos \phi_\alpha(t) - \dot{\theta}_\beta(t) \cos \phi_\beta(t) \quad (22)$$

with $0 \leq \theta_\alpha(t), \theta_\beta(t) \leq \pi$, $0 \leq \phi_\alpha(t), \phi_\beta(t) < 2\pi$. The constraints imposed by Eqs. (20) and (21) can be fulfilled by choosing $\dot{\phi}_\alpha(t) = \dot{\phi}_\beta(t) = 0$ so that the general solution of Eq. 22 is given by

$$\theta_\beta(t) = \theta_\beta(0) + \frac{\cos \phi_\alpha(0)}{\cos \phi_\beta(0)} \int_0^T dt \dot{\theta}_\alpha(t). \quad (23)$$

Apart from being integrable, the function $\dot{\theta}_\alpha(t)$ can be chosen arbitrarily. According to Eqs. (18), the time dependencies of the Rabi frequencies are given by

$$\begin{aligned}\Omega_1(t) &= -\dot{\theta}_\alpha(t) (\sin \phi_\alpha + \cos \phi_\alpha \tan \phi_\beta) \\ \Omega_2(t) &= 2\dot{\theta}_\alpha(t) \cos \phi_\alpha \\ \Omega_3(t) &= -\dot{\theta}_\alpha(t) (\sin \phi_\alpha - \cos \phi_\alpha \tan \phi_\beta).\end{aligned}\quad (24)$$

As the next step, we proceed to determine the initial and final values of the curve γ , i.e. $\{\boldsymbol{\alpha}(0), \boldsymbol{\beta}(0)\}$ and $\{\boldsymbol{\alpha}(T), \boldsymbol{\beta}(T)\}$. As the initially prepared W state is an eigenstate of $S_3 + T_3$ and $|\boldsymbol{\alpha}(t)| = |\boldsymbol{\beta}(t)| = \pi$ we can choose $\alpha_3(0) = \beta_3(0) = \pi$. Alternatively also the choice $\alpha_3(0) = \beta_3(0) = -\pi$ would have been possible. The final values of the curve γ at $t = T$ can be determined from the transformation properties explicitly worked out in Appendix A. For $|\boldsymbol{\alpha}(t)| = |\boldsymbol{\beta}(t)| = \pi$ they reduce to the conditions

$$\begin{aligned}\frac{\pi^2}{\sqrt{2}} &= |\alpha_3(T)\beta_2(T) + \alpha_2(T)\beta_3(T)|, \\ 0 &= \alpha_1(T)\beta_1(T) + \alpha_2(T)\beta_2(T) - \alpha_3(T)\beta_3(T), \\ 0 &= \alpha_1(T)\beta_3(T) + \alpha_3(T)\beta_1(T), \\ \frac{\pi^2}{\sqrt{2}} &= |\alpha_2(T)\beta_1(T) - \alpha_1(T)\beta_2(T)|.\end{aligned}\quad (25)$$

Numerical solutions of these equations, which are consistent with the anholonomic boundary condition of Eq. (23), are presented in Table I of Appendix B. For completeness, let us mention that the inverse conversion from a GHZ- to a W state is easily realized through a time-reversal of the curve γ . Such a time reversal formally corresponds to interchanging $t = 0$ and $t = T$ in Eq. (23) and can practically be achieved using Rabi frequencies of the same magnitude as those in Eq. (24), but with the opposite sign.

Depending on the choice of the function $\dot{\theta}_\alpha(t)$ in Eq. (23) different time-dependent Rabi frequencies of the Hamiltonian (3) can enable the desired quantum state conversion from a W to a GHZ state. One of the simplest choices for $\dot{\theta}_\alpha(t)$ is a constant function which yields

$$\theta_\alpha(t) = t \frac{\theta_\alpha(T)}{T}, \quad t \in [0, T], \quad (26)$$

where in writing the last equation use has been made of the fact that $\theta_\alpha(0) = 0$. According to Eqs. (24) it gives rise to time independent Rabi frequencies corresponding to an instantaneous turn on and turn off of the laser pulses inducing these Rabi frequencies at $t = 0$ and $t = T$. Another possible choice for $\dot{\theta}_\alpha(t)$ is

$$\dot{\theta}_\alpha(t) = \frac{\theta_\alpha(T)}{T(1-\tau)} \begin{cases} t/(\tau T), & 0 \leq t \leq \tau T \\ 1, & \tau T \leq t \leq T - \tau T \\ (T-t)/(\tau T), & T - \tau T \leq t \leq T \end{cases} \quad (27)$$

which yields (continuous) Rabi frequencies vanishing at $t = 0$ and at $t = T$ and being turned on and off during a time interval of duration τT .

In Figs. 2 and 3 characteristic features of the quantum state conversion from a W to a GHZ state resulting from these two types of time dependent Rabi frequencies are compared with the corresponding results of the recently proposed STA-based scheme of Ref. [17] which is based on the Lewis-Riesenfeld (LR) theory. For this comparison the Rabi frequencies of these different quantum state conversion schemes are normalized such that their total squared pulse areas, i.e.

$$A(t) = \int_0^t \sum_{i=3}^3 \Omega_i^2(t') dt', \quad (28)$$

are equal for times t that correspond to the total pulse durations ($t = T_{\min}$ and $t = T_{\text{LR}}$, respectively). This implies that in all these schemes the same (time averaged) laser energy is required for achieving the quantum state conversion. In particular, we elect to normalize them to the total squared pulse area A_{LR} corresponding to the LR scheme [cf. Fig. 2(b)].

The time evolution of the three Rabi frequencies capable of converting a W state to a GHZ state according to Eq. (27) with parameters $\theta_\alpha(T) = 1.92423$, $\theta_\beta(T) = 0.906373$, $q_1 = q_3 = 1$, $q_2 = -1$ are depicted by the solid lines in Fig. 2(a). In this example the relative turn-on and turn-off time τ [cf. Eq. (27)] of these time-dependent Rabi frequencies has been chosen as one third of the total pulse duration (i.e. $\tau = 1/3$). These time-dependent Rabi frequencies are compared with the recently proposed pulse sequences resulting from a LR invariant [17] (dashed lines). All Rabi frequencies, in both our approach and in that of Ref. [17], are assumed to vanish outside of their respective time interval $[0, T]$. Time is plotted in units of the time T_{LR} which is required to complete the state conversion $|W\rangle \rightarrow |\text{GHZ}\rangle$ in the LR scheme. It is apparent from Fig. 3 that the time-dependent Rabi frequencies resulting from Eq. (27) are capable of completing the quantum state conversion in a significantly shorter time close to T_{\min} than the ones based on the LR scheme. The minimal conversion time T_{\min} is achieved with time-independent Rabi frequencies ($\tau = 0$) described by Eq. (26). The time evolutions of the GHZ-state fidelities $F_{\text{GHZ}} = |\langle \text{GHZ} | \psi(t) \rangle|$ corresponding

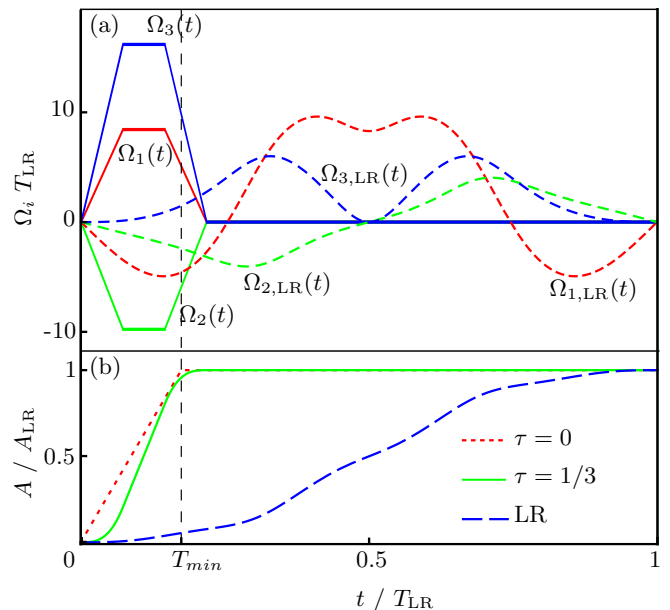


FIG. 2. (Color online)(a) Time evolution of Rabi frequencies for converting a W to a GHZ state, compared to the pulse sequences of the LR scheme of Ref. [17]. (b) Total squared pulse areas $A(t)$ [cf. Eq. (28)] for different pulse sequences: T_{LR} is the time required for the desired W -to-GHZ state conversion in the LR scheme, while T_{\min} is the corresponding time in the case of time-independent Rabi frequencies ($\tau = 0$).

to the pulse sequences shown in Fig. 2 are depicted in Fig. 3. Again the total squared pulse areas are equal for all three cases shown, namely the case of constant Rabi frequencies ($\tau = 0$), Rabi frequencies turned on and off during one third of the pulse duration ($\tau = 1/3$), and the Rabi frequencies of the LR scheme from Ref. [17].

In the system at hand – as usual for optical experiments in general – deleterious effects of decoherence are unavoidable. For instance, laser manipulation of atomic

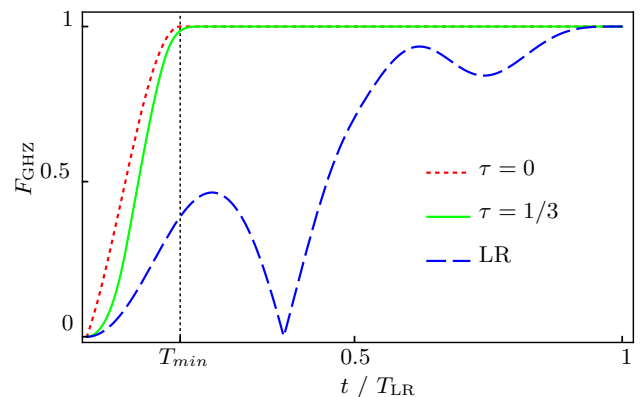


FIG. 3. (Color online) Time evolution of the GHZ-state fidelity $F_{\text{GHZ}} = |\langle \text{GHZ} | \psi(t) \rangle|$ for the pulse sequences displayed in Fig. 2.

states leads to phases that depend on atomic positions. Therefore, atomic motion inevitably gives rise to dephasing. Another important effect in the presence of laser excitation is spontaneous emission, which represents a major relaxation channel in the system under consideration. In what follows, we briefly discuss these decoherence processes within the framework of a Lindblad master equation [60]. We show that – for realistic values of the parameters that describe them – such imperfections have only a small effect on the fidelities of GHZ states resulting from our proposed state-conversion protocol.

In order to describe spontaneous emission originating from radiative decay, for example, the Lindblad operator

$$L_{\text{Sp}} = \sqrt{\Gamma} \sum_{n=1}^N |g\rangle_{nn} \langle r| \quad (29)$$

is used. It describes the spontaneous decay of individual atoms from the Rydberg- to the ground state, with Γ being the corresponding decay rate. Analogously, the operator

$$L_{\text{De}} = \sqrt{\gamma} \sum_{n=1}^N (|g\rangle_{nn} \langle g| - |r\rangle_{nn} \langle r|) \quad (30)$$

describes dephasing of Rydberg- and ground states with the dephasing rate γ . Using the full interaction Hamiltonian of the system [cf. Eq. (1)] and taking $\rho(0) = |W\rangle\langle W|$ as the initial state of the system at $t = 0$, we solve the corresponding Lindblad master equation numerically [61] and evaluate the resulting (open-system) fidelity with respect to the GHZ state

$$|\text{GHZ}\rangle_{\text{Int}} = \frac{1}{\sqrt{2}} \left(|ggg\rangle + e^{i(\varphi - \Delta E t/\hbar)} |rrr\rangle \right) \quad (31)$$

with

$$\Delta E/\hbar = 3V - \left(\frac{3\Omega_{r0}^2}{\Delta_0} + \frac{3\Omega_{r0}^2}{\Delta_0 - 2V} \right). \quad (32)$$

The time-dependent phase involving ΔE compensates for the fact that the GHZ state defined in Eq. (19) and the effective Hamiltonian of Eq. (3) refer to an interaction picture in which the energy shifts originating from the interatomic interaction and from the strong laser field with Rabi frequency Ω_{r0} have been taken into account whereas the Hamiltonian of Eq. (1) and the GHZ-state of Eq. (31) refer to an interaction picture without these energy shifts.

To demonstrate the robustness of our state-conversion protocol against decoherence (for an illustration, see Fig. 4), we investigate the open-system dynamics for the case of rather strong decoherence and dissipation with parameters $\Gamma = \gamma = 0.1/T_{\text{LR}}$, $T_{\text{LR}}\Omega_{r0} = 500$, $T_{\text{LR}}V = 2\pi \times 1000$, and $T_{\text{LR}}\Delta_0 = -2\pi \times 3000$. Figure 4 compares the obtained GHZ-state fidelities for our time-independent scheme ($\tau = 0$) and the one of Ref. [17] (LR), showing at the same time the results obtained in

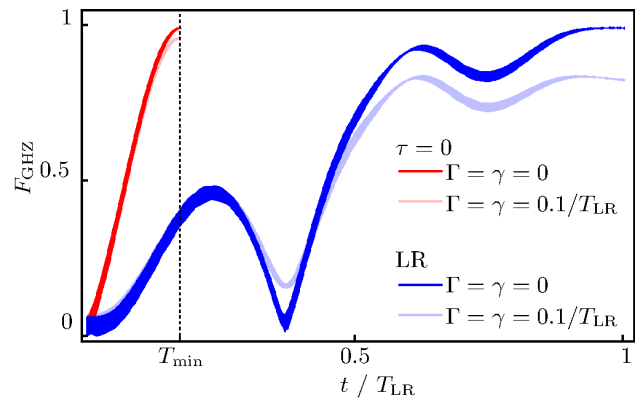


FIG. 4. (Color online) Time evolution of the GHZ-state fidelity F_{GHZ} in the open system approach for our time-independent pulse sequences and for the pulse sequences of the LR scheme of Ref. [17].

the closed-system scenario ($\Gamma = \gamma = 0$) for both of these schemes. Because our scheme allows one to carry out the desired state conversion in a significantly shorter time, its corresponding GHZ-state fidelity is much less affected by decoherence, as its deleterious effects accumulate over time. Even with the above values for the decoherence and dissipation rates Γ and γ , our scheme still preserves a fidelity that exceeds 96% for $t \approx T_{\text{min}}$. [Note that the broadening of the lines in Fig. 4 is a consequence of small oscillations, which are not taken into account in the rotating-wave approximation used for the derivation of the effective Hamiltonian of Eq. (3) and which could be minimized by choosing an even larger detuning Δ_0 .]

Owing to the advanced experimental capabilities currently available, even an application of complex time-dependent laser pulses of the kind obtained in Ref. [17] is in principle feasible. Yet, our scheme – with its resulting time-independent Rabi frequencies – is more easily applicable experimentally, especially from the standpoint of scaling to larger systems. As can be inferred from Fig. 3, an important additional advantage of our scheme – compared to that of Ref. [17] – is that the time T_{min} it requires for the conversion of a W state into its GHZ counterpart is significantly shorter than the corresponding time T_{LR} in Ref. [17].

VI. SUMMARY AND CONCLUSIONS

To summarize, in this paper we addressed the problem of W -to-GHZ state conversion in the Rydberg-blockade regime of a neutral atom system in which each atom is driven by four external laser pulses. While the same problem has recently been investigated using shortcuts to adiabaticity – more precisely, techniques based on Lewis-Riesenfeld invariants [17] – we have treated it using a completely different, Lie-algebraic approach based on the dynamical symmetries of the underlying system.

Because it employs Lie-algebraic techniques in the con-

text of quantum-state control, our work presents a significant degree of novelty from the methodological standpoint. Namely, the use of Lie-algebraic concepts in the realm of quantum control has heretofore been almost exclusively confined to the realm of quantum operator control [62, 63] – typically in the context of quantum-gate optimization [64, 65] – where they provide the mathematical underpinnings of the concept of complete controllability [62, 66].

Most importantly, our resulting state-conversion protocol has two principal advantages compared to that of Ref. [17]. Firstly, unlike the latter work, which leads to a state-conversion protocol involving strongly time-dependent Rabi frequencies of external lasers, our approach results in a significantly simpler one, which even allows for time-independent Rabi frequencies. Secondly, our approach allows the sought-after W -to-GHZ state conversion to be carried out significantly faster than that of Ref. [17]. Both of these advantages also speak in favour of an easier experimental implementation of our protocol, as well as its better scalability.

With minor modifications, our approach can be generalized, not only to other state-conversion problems in the Rydberg-atom system under consideration, but also to systems belonging to other QIP platforms. An experimental implementation of our state-conversion protocol is keenly anticipated.

ACKNOWLEDGMENTS

The authors acknowledge useful discussions with G. Birkel and A. R. P. Rau. This research was supported by the Deutsche Forschungsgemeinschaft (DFG) – SFB 1119 – 236615297.

Appendix A: Unitary transformations of the pseudospin states in Eqs. (10) and (11)

We consider a general unitary transformation as defined by Eq. (12). From the four-dimensional representation of the angular-momentum operators S_i and T_i [cf. Eq. (5)], it is straightforward to obtain the relations

$$\begin{aligned} e^{-i\boldsymbol{\alpha}\cdot\mathbf{S}} &= \cos\frac{|\boldsymbol{\alpha}|}{2} - 2i\sin\frac{|\boldsymbol{\alpha}|}{2}\frac{\boldsymbol{\alpha}\cdot\mathbf{S}}{|\boldsymbol{\alpha}|}, \\ e^{-i\boldsymbol{\beta}\cdot\mathbf{T}} &= \cos\frac{|\boldsymbol{\beta}|}{2} - 2i\sin\frac{|\boldsymbol{\beta}|}{2}\frac{\boldsymbol{\beta}\cdot\mathbf{T}}{|\boldsymbol{\beta}|}. \end{aligned} \quad (\text{A1})$$

For the pseudospin states of Eqs. (10) and (11) the last two relations imply that

$$\begin{aligned} e^{-i\boldsymbol{\alpha}\cdot\mathbf{S}}|\uparrow\nu\rangle &= M_{++}(\boldsymbol{\alpha})|\uparrow\nu\rangle + M_{+-}(\boldsymbol{\alpha})|\downarrow\nu\rangle, \\ e^{-i\boldsymbol{\alpha}\cdot\mathbf{S}}|\downarrow\nu\rangle &= -M_{+-}^*(\boldsymbol{\alpha})|\uparrow\nu\rangle + M_{++}^*(\boldsymbol{\alpha})|\downarrow\nu\rangle \end{aligned} \quad (\text{A2})$$

where $\nu \in \{\uparrow, \downarrow\}$ and

$$\begin{aligned} M_{++}(\boldsymbol{\alpha}) &= \cos\frac{|\boldsymbol{\alpha}|}{2} - i\frac{\alpha_3}{|\boldsymbol{\alpha}|}\sin\frac{|\boldsymbol{\alpha}|}{2}, \\ M_{+-}(\boldsymbol{\alpha}) &= \frac{(-i\alpha_1 + \alpha_2)}{|\boldsymbol{\alpha}|}\sin\frac{|\boldsymbol{\alpha}|}{2}. \end{aligned} \quad (\text{A3})$$

In deriving the last results, use has been made of the fact that the angular-momentum operators S_i act on the first pseudospin only. Because $|M_{++}(\boldsymbol{\alpha})|^2 + |M_{+-}(\boldsymbol{\alpha})|^2 = 1$, for $\boldsymbol{\alpha} \in \mathbb{R}^3$, these unitary transformations belong to the group $SL(2, \mathbb{C})$.

By applying an additional unitary transformation generated by the angular-momentum operators T_j – which commute with S_i ($i, j \in \{1, 2, 3\}$) and act on the second pseudospin only – we finally obtain the following relations:

$$\begin{aligned} e^{-i\boldsymbol{\alpha}\cdot\mathbf{S}}e^{-i\boldsymbol{\beta}\cdot\mathbf{T}}|\uparrow\uparrow\rangle &\longrightarrow \\ \frac{1}{\sqrt{2}} \begin{pmatrix} -iM_{++}(\boldsymbol{\alpha})M_{++}(\boldsymbol{\beta}) - iM_{+-}(\boldsymbol{\alpha})M_{+-}(\boldsymbol{\beta}) \\ -iM_{++}(\boldsymbol{\alpha})M_{+-}(\boldsymbol{\beta}) - iM_{+-}(\boldsymbol{\alpha})M_{++}(\boldsymbol{\beta}) \\ M_{++}(\boldsymbol{\alpha})M_{++}(\boldsymbol{\beta}) - M_{+-}(\boldsymbol{\alpha})M_{+-}(\boldsymbol{\beta}) \\ -M_{++}(\boldsymbol{\alpha})M_{+-}(\boldsymbol{\beta}) + M_{+-}(\boldsymbol{\alpha})M_{++}(\boldsymbol{\beta}) \end{pmatrix}, \\ e^{-i\boldsymbol{\alpha}\cdot\mathbf{S}}e^{-i\boldsymbol{\beta}\cdot\mathbf{T}}|\downarrow\uparrow\rangle &\longrightarrow \\ \frac{1}{\sqrt{2}} \begin{pmatrix} -iM_{++}^*(\boldsymbol{\alpha})M_{+-}(\boldsymbol{\beta}) + iM_{+-}^*(\boldsymbol{\alpha})M_{++}(\boldsymbol{\beta}) \\ -iM_{++}^*(\boldsymbol{\alpha})M_{++}(\boldsymbol{\beta}) + iM_{+-}^*(\boldsymbol{\alpha})M_{+-}(\boldsymbol{\beta}) \\ -M_{++}^*(\boldsymbol{\alpha})M_{+-}(\boldsymbol{\beta}) - M_{+-}^*(\boldsymbol{\alpha})M_{++}(\boldsymbol{\beta}) \\ M_{++}^*(\boldsymbol{\alpha})M_{++}(\boldsymbol{\beta}) + M_{+-}^*(\boldsymbol{\alpha})M_{+-}(\boldsymbol{\beta}) \end{pmatrix}, \\ e^{-i\boldsymbol{\alpha}\cdot\mathbf{S}}e^{-i\boldsymbol{\beta}\cdot\mathbf{T}}|\uparrow\downarrow\rangle &\longrightarrow \\ \frac{1}{\sqrt{2}} \begin{pmatrix} iM_{++}(\boldsymbol{\alpha})M_{+-}^*(\boldsymbol{\beta}) - iM_{+-}(\boldsymbol{\alpha})M_{++}^*(\boldsymbol{\beta}) \\ -iM_{++}(\boldsymbol{\alpha})M_{++}^*(\boldsymbol{\beta}) + iM_{+-}(\boldsymbol{\alpha})M_{+-}^*(\boldsymbol{\beta}) \\ -M_{++}(\boldsymbol{\alpha})M_{+-}^*(\boldsymbol{\beta}) - M_{+-}(\boldsymbol{\alpha})M_{++}^*(\boldsymbol{\beta}) \\ -M_{++}(\boldsymbol{\alpha})M_{++}^*(\boldsymbol{\beta}) - M_{+-}(\boldsymbol{\alpha})M_{+-}^*(\boldsymbol{\beta}) \end{pmatrix}, \\ e^{-i\boldsymbol{\alpha}\cdot\mathbf{S}}e^{-i\boldsymbol{\beta}\cdot\mathbf{T}}|\downarrow\downarrow\rangle &\longrightarrow \\ \frac{1}{\sqrt{2}} \begin{pmatrix} -iM_{++}^*(\boldsymbol{\alpha})M_{++}^*(\boldsymbol{\beta}) - iM_{+-}^*(\boldsymbol{\alpha})M_{+-}^*(\boldsymbol{\beta}) \\ +iM_{++}^*(\boldsymbol{\alpha})M_{+-}^*(\boldsymbol{\beta}) + iM_{+-}^*(\boldsymbol{\alpha})M_{++}^*(\boldsymbol{\beta}) \\ -M_{++}^*(\boldsymbol{\alpha})M_{++}^*(\boldsymbol{\beta}) + M_{+-}^*(\boldsymbol{\alpha})M_{+-}^*(\boldsymbol{\beta}) \\ -M_{++}^*(\boldsymbol{\alpha})M_{+-}^*(\boldsymbol{\beta}) + M_{+-}^*(\boldsymbol{\alpha})M_{++}^*(\boldsymbol{\beta}) \end{pmatrix}. \end{aligned} \quad (\text{A4})$$

Appendix B: Parameters describing GHZ states

In order to determine the parameters $\{\boldsymbol{\alpha}(T), \boldsymbol{\beta}(T)\}$ which describe a GHZ state [as defined by Eq. (19)], we start from its expansion in terms of the orthonormal basis states of Eqs. (10) and (11), i.e.

$$|\text{GHZ}\rangle = \frac{1}{2} (i|\uparrow\uparrow\rangle + i|\downarrow\downarrow\rangle + e^{i\varphi}|\downarrow\uparrow\rangle - e^{i\varphi}|\uparrow\downarrow\rangle). \quad (\text{B1})$$

$\theta_\alpha(T)$	$\theta_\beta(T)$	$\phi_\alpha(0)$	$\phi_\beta(0)$	q_1	q_2	q_3
1.92423	0.906373	4.33454	2.47062	+1	-1	+1
1.92423	0.906373	1.94864	3.81256	+1	+1	+1
1.92423	0.906373	1.19295	5.61221	-1	+1	+1
1.92423	0.906373	5.09024	0.670972	-1	-1	+1
0.906373	1.92423	2.47062	4.33454	-1	+1	-1
0.906373	1.92423	3.81256	1.94864	-1	-1	-1
0.906373	1.92423	5.61221	1.19295	-1	-1	-1
0.906373	1.92423	0.670972	5.09024	+1	+1	-1

TABLE I. Spherical coordinates in the parameter space of the Lie algebra $su(2) \oplus su(2)$ describing GHZ states as defined by Eq.(19).

With the aid of Eqs. (A4) we obtain the relations

$$\begin{aligned}
\pm \frac{1}{\sqrt{2}} &= -\Im (M_{++}(\alpha(T))M_{+-}^*(\beta(T))) + \\
&\quad \Im (M_{+-}(\alpha(T))M_{++}^*(\beta(T))), \\
0 &= \Re (M_{++}(\alpha(T))M_{++}^*(\beta(T))) - \\
&\quad \Re (M_{+-}(\alpha(T))M_{+-}^*(\beta(T))), \\
0 &= \Re (M_{++}(\alpha(T))M_{+-}^*(\beta(T))) + \\
&\quad \Re (M_{+-}(\alpha(T))M_{++}^*(\beta(T))), \\
\pm \frac{1}{\sqrt{2}} &= \Im (M_{++}(\alpha(T))M_{++}^*(\beta(T))) + \\
&\quad \Im (M_{+-}(\alpha(T))M_{+-}^*(\beta(T))) \quad (B2)
\end{aligned}$$

for the parameters of a GHZ state, where \Re (\Im) denotes the real (imaginary) part of a complex quantity.

In the special case of $|\alpha(T)| = |\beta(T)| = \pi$ these relations reduce to Eqs. (25)), whose general solutions are given by

$$\begin{aligned}
\alpha(T) &\rightarrow \begin{pmatrix} q_1 \alpha_3 \\ q_2 \sqrt{\pi^2 - 2\alpha_3^2} \\ \alpha_3 \end{pmatrix}, \\
\beta(T) &\rightarrow \begin{pmatrix} -q_1 q_3 \sqrt{\pi^2 - 2\alpha_3^2} \\ 2q_2 q_3 \alpha_3 \\ q_3 \sqrt{\pi^2 - 2\alpha_3^2} \end{pmatrix} \quad (B3)
\end{aligned}$$

with $-\pi/\sqrt{2} \leq \alpha_3 \leq \pi/\sqrt{2}$ and $q_1, q_2, q_3 \in \{-1, +1\}$. Introducing spherical coordinates yields the relations

$$\begin{aligned}
\cos \phi_\alpha(0) &= q_1 \cot \theta_\alpha(T), \\
\cos \phi_\beta(0) &= -q_1 \cot \theta_\beta(T), \\
\cos^2 \theta_\alpha(T) + \cos^2 \theta_\beta(T) &= \frac{1}{2} \quad (B4)
\end{aligned}$$

which have to be fulfilled necessarily by the spherical coordinates of a GHZ state. In addition, these coordinates have to fulfill the anholonomic boundary conditions of Eq.(23) relating $\theta_\beta(T)$ and $\theta_\alpha(T)$. This leads to a unique set of spherical coordinates for each combination of q_1, q_2, q_3 describing the desired state conversion. These sets are given explicitly in Table I.

-
- [1] F. Haas, J. Volz, R. Gehr, J. Reichel, and J. Esteve, *Science* **344**, 180 (2014).
[2] C. Song *et al.*, *Phys. Rev. Lett.* **119**, 180511 (2017).
[3] N. Friis, O. Marty, C. Maier, C. Hempel, M. Holzäpfel, P. Jurcevic, M. B. Plenio, M. Huber, C. Roos, R. Blatt *et al.*, *Phys. Rev. X* **8**, 021012 (2018).
[4] J. P. Dowling and G. J. Milburn, *Phil. Trans. R. Soc. A* **361**, 1655 (2003).
[5] W. P. Schleich, K. S. Ranade, C. Anton, M. Arndt, M. Aspelmeyer, M. Bayer, G. Berg, T. Calarco, H. Fuchs, E. Giacobino *et al.*, *Appl. Phys. B* **122**, 130 (2016).
[6] D. Barredo, S. de Léséleuc, V. Lienhard, T. Lahaye, and A. Browaeys, *Science* **354**, 1021 (2016).
[7] H. Bernien, S. Schwartz, A. Keesling, H. Levine, A. Omran, H. Pichler, S. Choi, A. S. Zibrov, M. Endres, M. Greiner, *et al.*, *Nature (London)* **551**, 579 (2017).
[8] D. Barredo, V. Lienhard, S. de Léséleuc, T. Lahaye, and A. Browaeys, *Nature (London)* **561**, 79 (2018).
[9] M. O. Brown, T. Thiele, C. Kiehl, T.-W. Hsu, and C. A. Regal, *Phys. Rev. X* **9**, 011057 (2019).
[10] D. Ohl de Mello, D. Schäffner, J. Werkmann, T. Preuschoff, L. Kohfahl, M. Schlosser, and G. Birkel, *Phys. Rev. Lett.* **122**, 203601 (2019).
[11] K.-N. Schymik, V. Lienhard, D. Barredo, P. Scholl, H. Williams, A. Browaeys, and T. Lahaye, *Phys. Rev. A* **102**, 063107 (2020).

- [12] T. F. Gallagher, *Rydberg Atoms* (Cambridge University Press, Cambridge, 1994).
- [13] For an up-to-date review, see C. S. Adams, J. D. Pritchard, and J. P. Shaffer, *J. Phys. B: At. Mol. Opt. Phys.* **53**, 012002 (2020).
- [14] L. F. Buchmann, K. Mølmer, and D. Petrosyan, *Phys. Rev. A* **95**, 013403 (2017).
- [15] M. Ostmann, J. Minář, M. Marcuzzi, E. Levi, and I. Lesanovsky, *New J. Phys.* **19**, 123015 (2017).
- [16] A. Omran, H. Levine, A. Keesling, G. Semeghini, T. T. Wang, S. Ebadi, H. Bernien, A. S. Zibrov, H. Pichler, S. Choi *et al.*, *Science* **365**, 570 (2019).
- [17] R.-H. Zheng, Y.-H. Kang, D. Ran, Z.-C. Shi, and Y. Xia, *Phys. Rev. A* **101**, 012345 (2020).
- [18] R. Mukherjee, H. Xie, and F. Mintert, *Phys. Rev. Lett.* **125**, 203603 (2020).
- [19] V. M. Stojanović, *Phys. Rev. A* **103**, 022410 (2021).
- [20] L. S. Theis, F. Motzoi, F. K. Wilhelm und M. Saffman, *Phys. Rev. A* **94**, 032306 (2016).
- [21] H. Levine, A. Keesling, A. Omran, H. Bernien, S. Schwartz, A. S. Zibrov, M. Endres, M. Greiner, V. Vuletić und M. D. Lukin, *Phys. Rev. Lett.* **121**, 123603 (2018).
- [22] M. Saffman, T. G. Walker, and K. Mølmer, *Rev. Mod. Phys.* **82**, 2313 (2010).
- [23] M. Saffman, *J. Phys. B* **49**, 202001 (2016).
- [24] For an up-to-date review, see, e.g., M. Morgado and S. Whitlock, arXiv:2011.03031.
- [25] W. Dür, G. Vidal, and J. I. Cirac, *Phys. Rev. A* **62**, 062314 (2000).
- [26] D. M. Greenberger, M. A. Horne, and A. Zeilinger, in *Bell's Theorem, Quantum Theory, and Conceptions of the Universe* (Kluwer Academic, Dordrecht, 1989), pp. 73-76.
- [27] M. A. Nielsen, *Phys. Rev. Lett.* **83**, 436 (1999).
- [28] J. Joo, Y.-J. Park, S. Oh, and J. Kim, *New J. Phys.* **5**, 136 (2003).
- [29] C. Zhu, F. Xu, and C. Pei, *Sci. Rep.* **5**, 17449 (2015).
- [30] V. Lipinska, G. Murta, and S. Wehner, *Phys. Rev. A* **98**, 052320 (2018).
- [31] T. Tashima, Ş. K. Özdemir, T. Yamamoto, M. Koashi, and N. Imoto, *Phys. Rev. A* **77**, 030302(R) (2008).
- [32] X. Peng, J. Zhang, J. Du, and D. Suter, *Phys. Rev. Lett.* **103**, 140501 (2009); *Phys. Rev. A* **81**, 042327 (2010).
- [33] A. A. Gangat, I. P. McCulloch, and G. J. Milburn, *Phys. Rev. X* **3**, 031009 (2013).
- [34] C. Li and Z. Song, *Phys. Rev. A* **91**, 062104 (2015).
- [35] Y.-H. Kang, Y.-H. Chen, Z.-C. Shi, J. Song, and Y. Xia, *Phys. Rev. A* **94**, 052311 (2016).
- [36] Y.-H. Kang, Y.-H. Chen, Q.-C. Wu, B.-H. Huang, J. Song, and Y. Xia, *Sci. Rep.* **6**, 36737 (2016).
- [37] B. Fang, M. Menotti, M. Liscidini, J. E. Sipe, and V. O. Lorenz, *Phys. Rev. Lett.* **123**, 070508 (2019).
- [38] V. M. Stojanović, *Phys. Rev. Lett.* **124**, 190504 (2020).
- [39] S. Bugu, F. Ozaydin, T. Ferrus, and T. Koder, *Sci. Rep.* **10**, 3481 (2020).
- [40] A. S. Coelho, F. A. S. Barbosa, K. N. Cassemiro, A. S. Villar, M. Martinelli, and P. Nussenzveig, *Science* **326**, 823 (2009).
- [41] M. Erhard, M. Malik, M. Krenn, and A. Zeilinger, *Nat. Photon.* **12**, 759 (2018).
- [42] V. Macrì, F. Nori, and A. Frisk Kockum, *Phys. Rev. A* **98**, 062327 (2018).
- [43] R.-H. Zheng, Y.-H. Kang, Z.-C. Shi, and Y. Xia, *Ann. Phys. (Berlin)* **531**, 1800447 (2019).
- [44] P. Walther, K. J. Resch, and A. Zeilinger, *Phys. Rev. Lett.* **94**, 240501 (2005).
- [45] W. X. Cui, S. Hu, H. F. Wang, A. D. Zhu, and S. Zhang, *Opt. Express* **24**, 15319 (2016).
- [46] Y. H. Kang, Z. C. Shi, B. H. Huang, J. Song, and Y. Xia, *Phys. Rev. A* **100**, 012332 (2019).
- [47] J. Song, X. D. Sun, Q. X. Mu, L. L. Zhang, Y. Xia, and H. S. Song, *Phys. Rev. A* **88**, 024305 (2013).
- [48] G. Y. Wang, D. Y. Wang, W. X. Cui, H. F. Wang, A. D. Zhu, and S. Zhang, *J. Phys. B* **49**, 065501 (2016).
- [49] D. Tong *et al.*, *Phys. Rev. Lett.* **93**, 063001 (2004); K. Singer *et al.*, *ibid.* **93**, 163001 (2004).
- [50] E. Urban, T. A. Johnson, T. Henage, L. Isenhower, D. D. Yavuz, T. G. Walker, and M. Saffman, *Nature Phys.* **5**, 110 (2009); A. Gaëtan, Y. Miroshnychenko, T. Wilk, A. Chotia, M. Viteau, D. Comparat, P. Pillet, A. Browaeys, and P. Grangier, *ibid.* **5**, 115 (2009).
- [51] D. Guery-Odelin, A. Ruschhaupt, A. Kiely, E. Torrontegui, S. Martinez-Garaot, and J. G. Muga, *Rev. Mod. Phys.* **91**, 045001 (2019).
- [52] H. R. Lewis and W. B. Riesenfeld, *J. Math. Phys.* **10**, 1458 (1969).
- [53] M. D. Lukin, M. Fleischhauer, R. Cote, L. M. Duan, D. Jaksch, J. I. Cirac, and P. Zoller, *Phys. Rev. Lett.* **87**, 037901 (2001).
- [54] T. Wilk, A. Gaëtan, C. Evellin, J. Wolters, Y. Miroshnychenko, P. Grangier, and A. Browaeys, *Phys. Rev. Lett.* **104**, 010502 (2010).
- [55] L. Isenhower, E. Urban, X. L. Zhang, A. T. Gill, T. Henage, T. A. Johnson, T. G. Walker, and M. Saffman, *Phys. Rev. Lett.* **104**, 010503 (2010).
- [56] M. Saffman and K. Mølmer, *Phys. Rev. Lett.* **102**, 240502 (2009).
- [57] A. O. Barut, *Dynamical Groups and Generalized Symmetries in Quantum Theory (with applications in atomic and particle physics)* (University of Canterbury Publ., Christchurch, New Zealand, 1971).
- [58] See, e.g., A. R. P. Rau and G. Alber, *J. Phys. B: At. Mol. Opt. Phys.* **50**, 242001 (2017).
- [59] R. D. Richtmyer, *Principles of Advanced Mathematical Physics*, Vol. II (Springer, New York, 1981).
- [60] H.-P. Breuer and F. Petruccione, *The Theory of Open Quantum Systems* (Oxford University Press, 2002).
- [61] J. R. Johansson, P. D. Nation, and F. Nori, *Comput. Phys. Commun.* **183**, 1760 (2012); **184**, 1234 (2013).
- [62] V. Ramakrishna and H. Rabitz, *Phys. Rev. A* **54**, 1715 (1996).
- [63] R. Heule, C. Bruder, D. Burgarth, and V. M. Stojanović, *Phys. Rev. A* **82**, 052333 (2010); *Eur. Phys. J. D* **63**, 41 (2011).
- [64] V. M. Stojanović, A. Fedorov, A. Wallraff, and C. Bruder, *Phys. Rev. B* **85**, 054504 (2012).
- [65] E. Zahedinejad, J. Ghosh, and B. C. Sanders, *Phys. Rev. Lett.* **114**, 200502 (2015).
- [66] See, e.g., V. M. Stojanović, *Phys. Rev. A* **99**, 012345 (2019).